energies

MDPI

Article

Experimental Study on the Flow Characteristics of Two-Stage Variable Turbines in a Twin-VGT System

Qikai Peng [1,2], Zhongjie Zhang [2,*], Guangmeng Zhou [2], Surong Dong [2], Xumin Zhao [2], Han Zhang [1,2], Ruilin Liu [1,2] and Jun Cai [3]

[1] College of Power Engineering, Naval University of Engineering, Wuhan 430033, China; pengqikai@yeah.net (Q.P.)
[2] Military Vehicle Engineering Department, Army Military Transportation University, Tianjin 300161, China
[3] Jiangsu Kaidi Navigation Control System Limited Company, Wuxi 214161, China
* Correspondence: jjxyzzj@163.com

Abstract: The twin variable geometry turbocharger (VGT) System, through efficient use of exhaust energy, maximizes internal combustion engine (ICE) power, reduces exhaust emissions and improves reliability. However, the internal flow characteristics of the twin-VGT system are greatly affected by the environment. To ensure that the two-stage adjustable supercharged internal combustion engine is efficient in all geographical environments and under all operating conditions, it is necessary to conduct in-depth research on the internal flow characteristics of high- and low-pressure turbines. In this paper, an experimental system of the flow characteristics of a double variable-geometry turbocharging (twin-VGT) system is designed and developed. A two-stage variable turbine flow characteristic test was carried out, focusing on the relationship between the initial rotational velocity of high variable-geometry turbocharging (HVGT) and blade opening in low variable-geometry turbocharging (LVGT). The effects of high- and low-pressure variable-geometry turbocharger (VGT) blade opening on available exhaust energy, expansion ratio distribution, blade velocity ratio, compressor power consumption and isentropic efficiency were studied. The results show that when the available energy of exhaust gas is constant, with the increase in HVGT turbine speed, when the LVGT blade opening decreases by 10%, the low-pressure turbine expansion ratio increases by about 0.23.

Keywords: vane adjustment opening; twin-VGT system; experimental system; internal combustion engine

check for updates

Citation: Peng, Q.; Zhang, Z.; Zhou, G.; Dong, S.; Zhao, X.; Zhang, H.; Liu, R.; Cai, J. Experimental Study on the Flow Characteristics of Two-Stage Variable Turbines in a Twin-VGT System. *Energies* **2023**, *16*, 7873. https://doi.org/10.3390/en16237873

Academic Editor: Davide Astolfi

Received: 19 September 2023
Revised: 23 October 2023
Accepted: 6 November 2023
Published: 1 December 2023

Copyright: © 2023 by the authors. Licensee MDPI, Basel, Switzerland. This article is an open access article distributed under the terms and conditions of the Creative Commons Attribution (CC BY) license (https://creativecommons.org/licenses/by/4.0/).

1. Introduction

At present, most modern engines are equipped with turbocharging systems to increase the intake air density by recycling the exhaust energy to increase the internal combustion engine (ICE) power efficiently and rapidly [1]. However, the complex and changing geographical environment of China places higher demands on the supercharging system [2]. For example, under variable altitude conditions, affected by changes in air density and exhaust gas temperature, the turbocharging system suffers from reduced efficiency, narrower flow range and increased tendency to wheeze, resulting in a reduction in the plateau performance of the internal combustion engine [3]. This is because the matching characteristics of the supercharger and the internal combustion engine change in a variable-altitude environment, and a supercharger with good matching characteristics in the plains is prone to serious torque drop in the low-speed region, turbo hysteresis, loss of compressor efficiency and low exhaust energy utilization in the plateau region [4–6]. It can be seen that, on the premise of ensuring the efficiency of the booster system, broadening the operating environment of the booster system is a problem we must face.

To ensure that the supercharging system is efficient in all geographical environments and under all operating conditions, advanced variable air management systems such as

variable-geometry turbochargers (VGT), supercharging systems with exhaust gas bypass valves, and two-stage adjustable supercharging systems are gradually being applied to variable-altitude internal combustion engines. Compared with a single stage turbocharger, the dual-VGT two-stage adjustable turbocharging system achieves effective distribution of exhaust energy between the high- and low-pressure stages of the turbine by adjusting the blade opening in the high- and low-pressure stages of the VGT, indirectly controlling the turbocharger speed and achieving precise control of boost pressure and intake flow to improve the overall efficiency of the turbocharging system [7]. However, in the design process of turbochargers, emphasis is placed on single-stage efficiency, often considering a single design point and conducting VGT blade opening tests based on the assumption of steady flow. Insufficient research has been conducted on the internal relationship between the opening of high- and low-pressure VGT blades in a two-stage adjustable turbocharging system, as well as the impact of blade opening on the distribution of exhaust energy, turbine expansion ratio and compressor turbocharging ratio [8]. As a result, the two-stage adjustable turbocharging system has an increased tendency for compressor overspeed and blockage under different environmental conditions [9], and the turbocharger has problems such as overspeed and an excessive pressure ratio [10], seriously affecting the environmental adaptability of internal combustion engines.

Zhang Yangjun of Tsinghua University [11] compared and analyzed the fuel consumption rate of a diesel engine at 1000 r/min speed under full load based on three supercharging systems: a high-pressure VGT, a low-pressure VGT and a dual-VGT system. The results show that the low-pressure VGT cannot reduce the brake specific fuel consumption (BSFC) of the diesel engine. Dual-VGT systems with high-pressure stages and bypass valves provide optimal BSFC. VGT+VGT can integrate the advantages of TST and a single-VGT system, which is the development trend of a two-stage supercharging system for future vehicles [12]. The dual-VGT two-stage adjustable supercharging system has the characteristics of a high pressure ratio and wide flow rate, which can simultaneously achieve the high pressure ratio and high efficiency of the supercharging system [13]. Under variable altitude conditions, the dual-VGT two-stage adjustable supercharging system can effectively allocate turbine work to improve exhaust energy utilization efficiency according to altitude and working condition characteristics, determine the optimal supercharging ratio distribution and comprehensively improve the high-altitude power of the internal combustion engine while maintaining the low-altitude power [14]. However, the interaction between high- and low-pressure blades of the two-stage adjustable supercharging system and the influence mechanism of exhaust energy change on turbine efficiency, compressor pressure ratio distribution and turbine enthalpy drop distribution are still unclear. Although the synergistic effect of two VGT blades can meet the performance requirements of the pressurization system of the internal combustion engine with varying altitude and working conditions, the change of intake conditions causes the actual running line of the internal combustion engine to deviate from the matching running line of the pressurization system. Under the condition of variable altitude, mismatch will occur, resulting in significant decline in internal combustion engine performance indexes such as power performance and economy [15,16]. Therefore, it is necessary to study the turbine flow characteristics of the two-stage adjustable supercharging system in detail. With respect to the investigation of the internal relationship between high- and low-pressure blade openings and the influence of turbine flow characteristics caused by blade opening changes on exhaust energy, total boost ratio, total expansion ratio and boost ratio distribution, the research results are of guiding significance for optimizing the control strategy of VGT blades in variable-altitude two-stage adjustable supercharging systems.

At present, the research on the flow rate characteristics of supercharging systems at home and abroad mainly focuses on the adjustment of VGT blade opening or the bypass valve of a single-stage supercharging system. More attention is paid to the performance test of the whole machine, and the methods used are mostly theoretical analysis and analog simulation [17,18]. In order to improve the environmental adaptability of the internal com-

bustion engine and improve the matching characteristics of the supercharging system and the variable altitude of the internal combustion engine, it is urgent to carry out experimental research on the flow characteristics of the two-stage variable turbocharging system [19]. In view of this, this paper is based on a self-developed two-stage variable turbine flow characteristics test system. By fixing three HVGT initial speeds (60,000 r/min, 75,000 r/min and 95,000 r/min), the combustion chamber injection volume is kept constant. Then, by gradually reducing the LVGT blade opening (100%, 80%, 60% and 30%), the effects of high- and low-pressure supercharger blade opening on exhaust energy availability, turbine expansion ratio distribution, turbine blade speed ratio, compressor power consumption and isentropic efficiency of the supercharging system were investigated. This study provides theoretical guidance for broadening the operating altitude of the supercharging system, improving the utilization rate of exhaust energy, and improving the environmental adaptability of the supercharging system and the internal combustion engine.

2. Establishment of Dual-VGT Two-Stage Variable Turbine Flow Characteristics Test System

In this paper, a two-stage VGT variable turbine flow characteristic test system is designed and developed, and on this basis, a special test of two-stage variable turbine flow is carried out: to investigate the law of influence of VGT blade opening on exhaust available energy distribution, expansion ratio distribution, leaf speed ratio and turbine efficiency in high- and low-pressure stages and to provide a theoretical basis for the optimal matching of a variable-altitude two-stage adjustable supercharging system and an ICE engine.

2.1. Design of a Dual-VGT Two-Stage Variable Turbine Flow Characteristics Test System

The arrangement of the dual-VGT two-stage variable turbine flow characteristics test system designed and developed in this paper is shown in Figure 1. The test system includes a combustion chamber gas heating system, a lubricating oil system, a measurement and data acquisition system, a control system and a piping system. The partial physical components of the experimental system are shown in Figure 2, and the main structural parameters of the high- and low-pressure VGT are shown in Table 1. The performance parameters of the main measuring instruments are shown in Table 2.

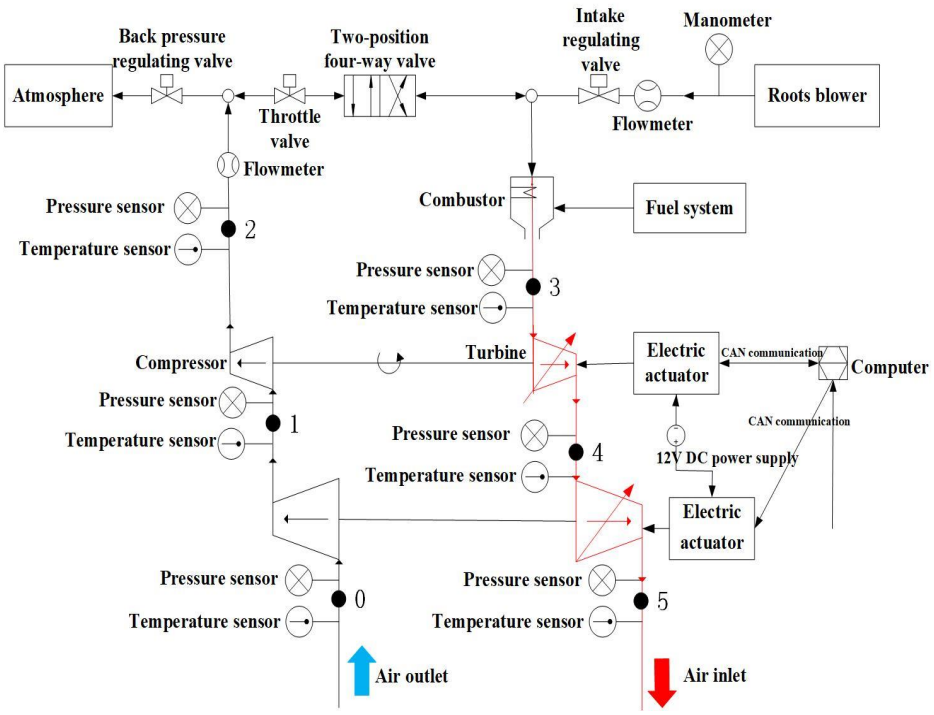


Figure 1. Double-VGT two-stage variable turbine flow characteristics test system.

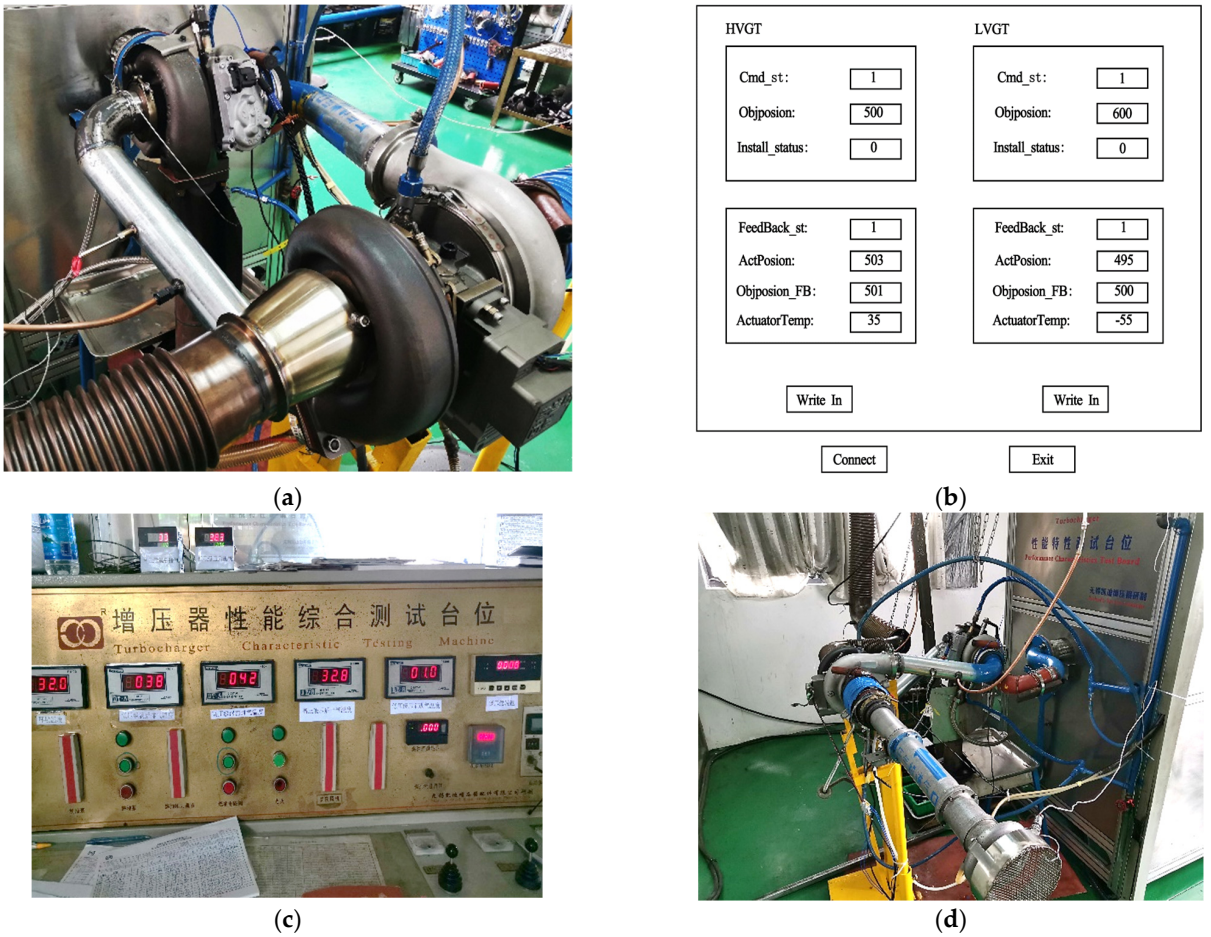


Figure 2. Double-VGT two-stage variable turbine flow characteristics test system and equipment physical drawing. (**a**) Dual-VGT two-stage adjustable supercharger. (**b**) Dual-VGT two-stage booster system actuator control interface. (**c**) Supercharger performance comprehensive control console. (**d**) Dual-VGT two-stage adjustable supercharging system.

Table 1. Main structural parameters of KD76GCT and KD100GCT turbochargers.

Turbocharger	Compressor Impeller Inlet Diameter/mm	Compressor Inlet Diameter/mm	Compressor Outlet Diameter/mm	Impeller Outlet Diameter/mm	Turbine Inlet Diameter/mm	Turbine Outlet Diameter/mm	Exhaust Pipe Diameter/mm
KD76GCT	52	52.8	62	76	74.5	60	61
KD100GCT	67	68	82.2	100	82	75	76

Table 2. Equipment information for testing and measurement.

Name (Quantity)	Model Number	Main Measurement Parameters	Measurement Accuracy
Pressure sensor (8)	Piezoresistive pressure sensor	Inlet and outlet air pressure of compressor and turbine	±0.5%
Pressure transmitter (2)	Electric transmitter	Compressor outlet pressure, turbine inlet pressure	±0.08% FS
Temperature sensor (4)	Platinum thermal resistance sensor	Inlet and outlet air temperature of compressor and turbine	±0.5 °C
Temperature transmitter (2)	Thermal resistance isolated transmitter	Compressor outlet air temperature, turbine inlet air temperature	±0.2%FS
Flow sensor (2)	Twisted-wire flowmeter	Compressor outlet flow, turbine inlet flow	>1%
Tachometer sensor (1)	Non-contact magnetoelectric	Turbocharger speed	≥±0.2%

Figure 3 shows the flow rate characteristics of the high- and low-pressure stage turbines for different VGT blade openings. The VGT blade opening of 100% represents the maximum position of the variable nozzle cross-section and the VGT blade opening of 0% represents the minimum position of the variable nozzle cross-section. The turbine similar flow rate ranges from 13.0 to 38.5 $\left(\mathrm{kg}\cdot\mathrm{k}^{\frac{1}{2}}\right)\cdot(\mathrm{s}\cdot\mathrm{kpa})^{-1}$, and the expansion ratio ranges from 1.25 to 3.60. When the VGT blade opening of the high- and low-pressure stage is 100%, the similar flow rate of the high- and low-pressure stage decreases as the VGT nozzle blade opening decreases. The turbine flow capacity of VGT blades at 40% opening is significantly lower than that at 60% or above blade opening, and the increment of turbine flow capacity between 40 and 60% blade opening is much larger than that between 60 and 80% opening. When the expansion ratio is 2.5, the similar flow rate for 40% blade opening in the high- and low-pressure stages is only 53% and 67% for 60% blade opening, while the similar flow rate for 60% blade opening is 82% and 78% for 100% blade opening.

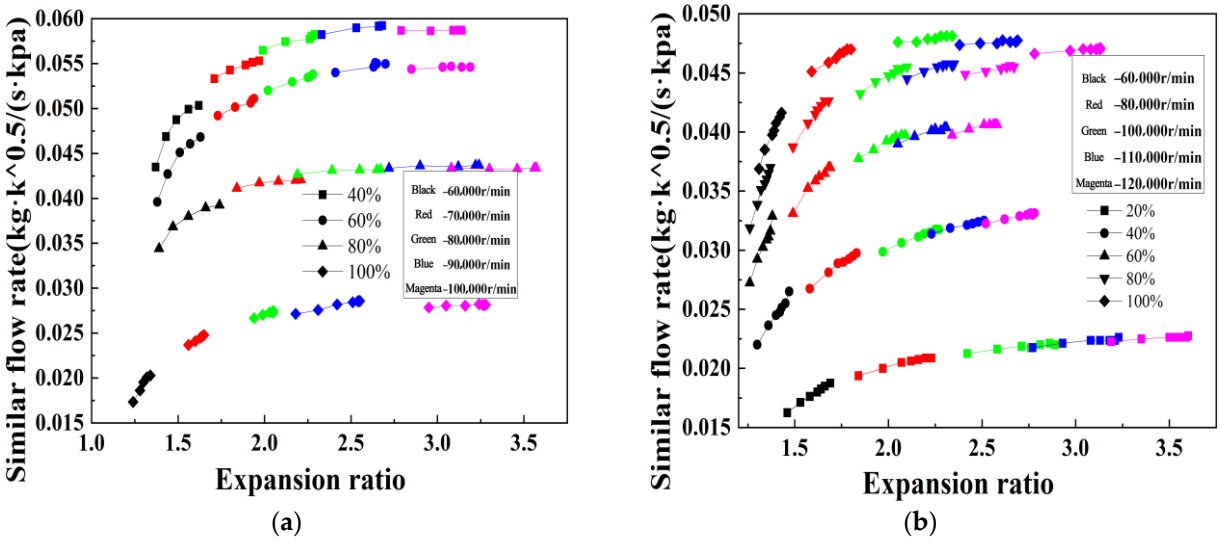


Figure 3. Two-stage turbine flow rate characteristic curve. (**a**) Low-pressure stage turbine (LT). (**b**) High-pressure stage turbine (HT).

The double-VGT two-stage variable turbine flow characteristic test was carried out according to JB/T9752.1-2005 [20], "Turbochargers Part 1: General Technical Conditions", and JB/T9752.2-2005 [21], "Turbochargers Part 2: Test methods". In order to meet the requirements of different engine working conditions, it is necessary to fix the initial HVGT speed to provide the best turbine speed under corresponding working conditions. The research finding that the optimum HVGT speed corresponding to low-speed working conditions, maximum-torque working conditions and calibrated-power working conditions, with respect to the working conditions of the engine, is 60,000 r/min, 75,000 r/min and 95,000 r/min. Considering that the selection of the LVGT blade opening should be representative, four typical blade openings of 100%, 80%, 60% and 30% were selected to cover the entire range of blade opening. In addition, a representative blade opening can be selected for accurate analysis according to specific characteristics during the experiment. In this paper, the test method is as follows: three HVGT initial speeds (60,000 r/min, 75,000 r/min and 95,000 r/min) are fixed, and the combustion chamber injection volume is kept constant. Then, the LVGT blade opening is gradually reduced (100%, 80%, 60% and 30%) to study the influence of VGT blade opening on the exhaust available energy, total expansion ratio, total boost ratio and expansion ratio distribution in high- and low-pressure stages. The secondary supercharger test adjustment conditions are shown in Table 3.

Table 3. Double-VGT two-stage adjustable supercharger test conditions.

Test Conditions	HVGT Vane Adjustment Opening (%)	LVGT Vane Adjustment Opening (%)	Initial Speed of High-Pressure Stage (r/min)	Low-Pressure Stage RPM(r/min)
A	100%	30%, 60%, 80%, 100%	60,000, 75,000, 95,000	Adjust the burner pressure, temperature and flow rate to increase the low-pressure stage speed, so that the low-pressure stage speed is stable to 50,000~100,000.
B	100%	30%, 60%, 80%, 100%	60,000, 75,000, 95,000	
C	100%	30%, 60%, 80%, 100%	60,000, 75,000, 95,000	
D	100%	30%, 60%, 80%, 100%	60,000, 75,000, 95,000	
E	100%	30%, 60%, 80%, 100%	60,000, 75,000, 95,000	
F	100%	30%, 60%, 80%, 100%	60,000, 75,000, 95,000	
A1	80%	30%, 60%, 80%, 100%	60,000, 75,000, 95,000	
B1	80%	30%, 60%, 80%, 100%	60,000, 75,000, 95,000	
C1	80%	30%, 60%, 80%, 100%	60,000, 75,000, 95,000	
D1	80%	30%, 60%, 80%, 100%	60,000, 75,000, 95,000	
E1	80%	30%, 60%, 80%, 100%	60,000, 75,000, 95,000	
F1	80%	30%, 60%, 80%, 100%	60,000, 75,000, 95,000	
A2	60%	30%, 60%, 80%, 100%	60,000, 75,000, 95,000	
B2	60%	30%, 60%, 80%, 100%	60,000, 75,000, 95,000	
C2	60%	30%, 60%, 80%, 100%	60,000, 75,000, 95,000	
D2	60%	30%, 60%, 80%, 100%	60,000, 75,000, 95,000	
E2	60%	30%, 60%, 80%, 100%	60,000, 75,000, 95,000	
F2	60%	30%, 60%, 80%, 100%	60,000, 75,000, 95,000	
A3	30%	30%, 60%, 80%, 100%	60,000, 75,000, 95,000	
B3	30%	30%, 60%, 80%, 100%	60,000, 75,000, 95,000	
C3	30%	30%, 60%, 80%, 100%	60,000, 75,000, 95,000	
D3	30%	30%, 60%, 80%, 100%	60,000, 75,000, 95,000	
E3	30%	30%, 60%, 80%, 100%	60,000, 75,000, 95,000	
F3	30%	30%, 60%, 80%, 100%	60,000, 75,000, 95,000	

The test process is as follows: First, determine the engine working conditions (low-speed conditions, maximum-torque conditions and calibrated-power conditions corresponding to speeds of 1000 r/min, 1500 r/min and 2100 r/min); and then, through the fuel system, fix the engine speed and keep the fuel injection amount unchanged. The initial HVGT speed and blade opening are then entered into the dual-VGT two-stage booster actuator control interface. At the beginning of the test, the LVGT blade opening is always maintained at 100%, and the LVGT blade opening is adjusted after the test system is stable. Until the pressurization system and engine operating conditions are stable, data are collected by sensors and stored in the data acquisition system (LC inlet pressure and temperature, HC inlet pressure and temperature, pressure and temperature of HC after supercharging, pressure and temperature in front of HT, pressure and temperature in front of LT, pressure and temperature behind the LT, HT/LT speed, compressor outlet flow and turbine intake flow rate). Finally, the blade opening of the LVGT is controlled by the supercharger control system, and the working characteristics of the two-stage adjustable supercharger system under different speeds and blade openings are obtained.

2.2. Calibration of the Cross-Section Position of the Variable Nozzle of the Secondary Turbine

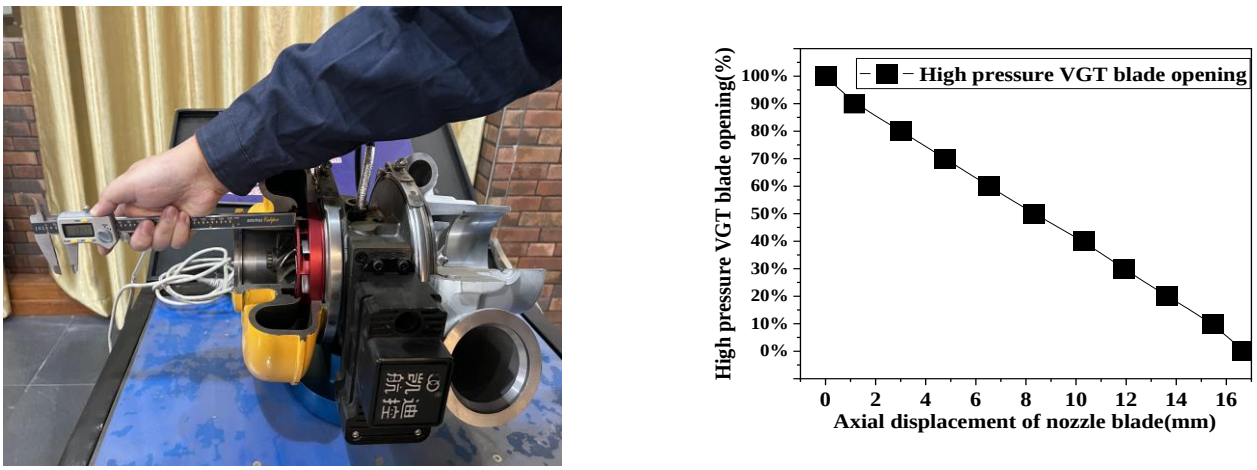
In this paper, both of the two-stage turbine's nozzle rings use an axial displacement structure to improve the reliability of VGT blade control. The motor drives the nozzle ring

blade with a gear. The mechanical transmission data for the variable cross-section nozzle movable blade travel and the rotation angle of the electronically controlled actuator motor are shown in Table 4.

Table 4. Stroke parameters of variable section nozzle blade of KD100GCT.

Parameter / Blade Stroke	Blade Stroke Range (mm)	Sector Gear Angle Range (°)	Blade Displacement Per Unit Sector Gear Angle (mm/°)	Blade Displacement Per Unit Motor Angle (mm/°)
Effective working stroke of nozzle moving blade	0~15	0~18.4	0.813	0.00769
Theoretical maximum stroke of nozzle moving blade	0~16.5	0~20.3		

To achieve precise control of the VGT blade opening, calibration of variable nozzle sections for high- and low-pressure stages was carried out, as shown in Figure 4a. The axial displacement of the nozzle section was calibrated using vernier calipers. Control of the axial displacement of the VGT nozzle cross-section was conducted from 10 to 100% via CAN bus.



(**a**) (**b**)

Figure 4. Calibration process of variable nozzle section for high-pressure turbines. (**a**) Axial displacement calibration of nozzle ring cross-section. (**b**) Relationship between nozzle ring axial displacement and VGT blade opening degree.

The position of the axial displacement of 0 mm corresponds to the full opening of the nozzle ring blade, and the opening of the VGT blade is defined as 100%. The position of the axial displacement of 16.68 mm corresponds to the complete closure of the nozzle ring blade, and the opening of the VGT blade is defined as 0%. Measurement of the actual distance of the corresponding axial displacement and plotting of the curve is shown in Figure 4b. As can be seen in the figure, the axial displacement of the nozzle blade of the high-pressure stage ranges from 0 mm to 16.68 mm. VGT opening and nozzle ring cross-section displacement exhibits a linear law of change, where linear error is less than 2%, and complete VGT blade opening calibration works.

3. Experimental Study on Flow Characteristics of Two VGT Two-Stage Variable Turbines

The geometric flow area of high- and low-stage turbines is determined by the combination of the nozzle ring cross-sectional area and the turbine impeller outlet area [22]. The adjustment of VGT blade opening changes the geometric through-flow area of the turbine by adjusting the flow area of the nozzle ring, and then adjusts the through-flow characteristics of high- and low-pressure turbines.

3.1. Effect of High- and Low-Pressure Stage VGT Blade Opening on the Distribution of Exhaust Available Energy and Expansion Ratio

According to the double-VGT two-stage variable turbine flow characteristics test system, the test analysis was conducted. Determination of the isentropic specific enthalpy of exhaust between cylinder exhaust state 3 and two-stage turbines' low-pressure stage exhaust state 5 was calculated as shown in Formula (1):

$$\Delta h_{(3\sim5)adT} = \frac{k_T R T_3^*}{k_T - 1}\left[1 - \left(\frac{1}{\pi_T}\right)^{\frac{k_T-1}{k_T}}\right] \quad (1)$$

In the formula, Δh_{adT} is the isentropic enthalpy drop of the turbine at 1 kg exhaust ((J/kg). k_T is the exhaust adiabatic index. T_3^* is the cylinder exhaust temperature. R is the gas constant (J/(kg·K)). π_T is the total expansion ratio of the two-stage turbine. From Formula (1), it can be seen that the exhaust available energy is mainly affected by the exhaust mass flow rate, vortex front exhaust temperature and expansion ratio. The influence laws for the degree of HVGT and LVGT blade opening on the distribution of vortex front exhaust temperature and expansion ratio are investigated separately below.

When the initial HVGT speed is =75,000 r/min, the available energy of high- and low-pressure exhaust gas varies with the VGT blade opening, as shown in Figure 5a. The pre-turbine temperature of the high-pressure stage increases with increasing HVGT blade opening. This is because as the HVGT blade opening decreases, the intake air volume increases, combustion in the combustion chamber is full and the exhaust gas temperature decreases. Different degrees of LVGT blade opening affect the available exhaust energy of the high-pressure stage to different degrees, and the available exhaust energy of the high-pressure stage increases as the LVGT blade opening decreases. This is because, as the LVGT opening decreases the back pressure behind the high-pressure stage vortex increases, and both the pressure and temperature in front of the high-pressure stage vortex increase. The variation trend of available exhaust energy for low-pressure turbines is the same as that for high-pressure turbines. This is due to the limited temperature drop of the high-pressure stage turbine, with an average temperature reduction of about 150 K (as shown in Figure 5b).

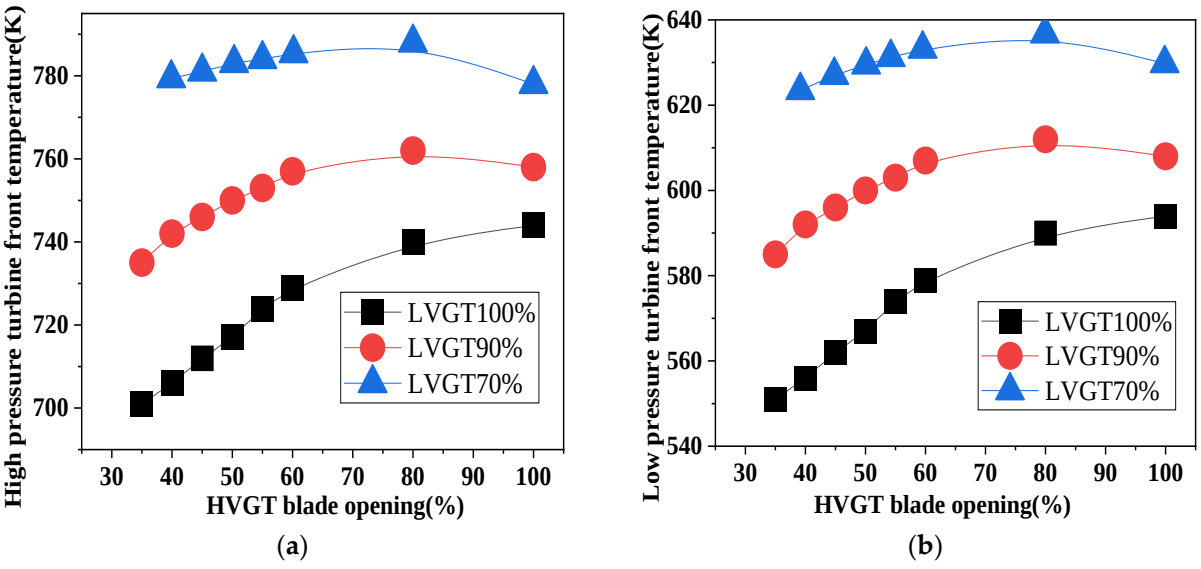


Figure 5. When the initial speed of HVGT = 75,000 r/min, the front exhaust temperature of high- and low-pressure turbines changes with the degree of VGT blade opening. (**a**) High-pressure stage turbine front temperature. (**b**) Low-pressure stage turbine front temperature.

At present, a lot of studies have been conducted on the control of exhaust energy in two-stage turbocharging systems through bypass valves and waste gates [23,24]. Among

them, regulating the exhaust energy through the high-pressure bypass valve is the most widely used structure at this stage. Only when the high-pressure stage turbine is completely bypassed, the low-pressure stage turbine is controlled with waste gates to adjust the boost pressure. But the above method easily wastes a lot of the available exhaust energy. The dual-VGT two-stage adjustable supercharging system optimizes the available energy utilization rate of exhaust gas by adjusting the VGT blade opening and achieves the high-pressure ratio and high efficiency of the supercharging system under different environmental conditions and different internal combustion engine working conditions. Therefore, it is of great practical value to study the coupling of flow characteristics of high- and low-pressure turbines with the available energy of the exhaust gas [25].

When the initial speed of the HVGT = 60,000 r/min, the expansion ratio of high- and low-pressure stage turbines varies with the blade opening of HVGT and LVGT, as shown in Figure 6. Where the high-pressure stage expansion ratio decreases with an increasing HVGT blade opening (shown in Figure 6a). The degree of HVGT blade opening plays a major role in the magnitude of the expansion ratio of the high-pressure stage compared to the degree of LVGT blade opening. Meanwhile, compared with the HVGT blades in the range of 100% to 60% openness, the trend for the turbine expansion ratio change in the high-pressure stage is more obvious in the range of 60% to 30% openness of the HVGT blades. Figure 6b shows that the degree of HVGT blade opening affects the low-pressure stage turbine expansion ratio to a small extent, and the low-pressure stage turbine expansion ratio increases by about 0.6 when the LVGT is reduced from 100% to 30%.

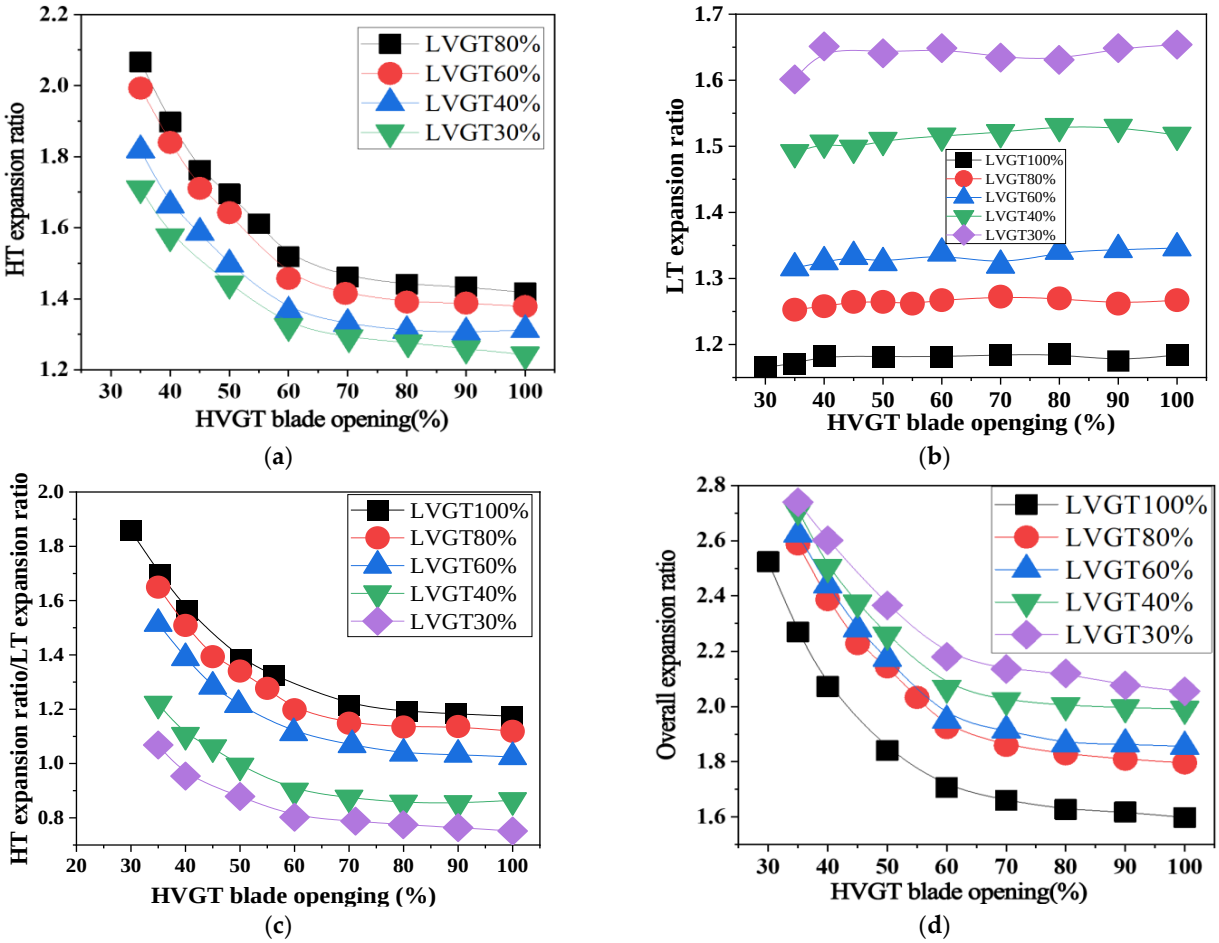


Figure 6. When the initial speed of HVGT is 60,000 r/min, the expansion ratio distribution of high- and low-pressure turbines varies with the opening of VGT blades. (**a**) HT expansion ratio. (**b**) LT expansion ratio. (**c**) Ratio of turbine expansion ratios for high- and low-pressure stages. (**d**) Total expansion ratio of turbine.

Figure 6c shows the relationship between the distribution of the turbine expansion ratios of the high- and low-pressure stages in relation to the variation of the HVGT and LVGT blade openings. From the figure, it can be seen that with LVGT blade openings of 100% to 60%, the turbine expansion ratio of the high-pressure stage decreases and the turbine expansion ratio of the low-pressure stage increases as the HVGT blade opening increases, but it is still greater than one. As the LVGT blade opening decreases, the low-pressure stage turbine expansion ratio increases. When the degree of LVGT blade openness is between 40% and 30%, as the HVGT blade opening increases, π_{HT}/π_{LT} decreases, and the value of π_{HT}/π_{LT} is less than 1 when the HVGT blade opening is greater than 60%. In Figure 6d, the total expansion ratio of the two-stage turbine shows an increasing trend with decreasing HVGT and LVGT blade openings. In the range of HVGT blade openness from 60% to 100%, the LVGT blade openings have a higher weighting of influence on the total expansion ratio. With HVGT blade opening in the range of 30% to 60%, the total expansion ratio of the two-stage turbine increases rapidly as the HVGT blade opening decreases, and the HVGT has a greater effect on the total expansion ratio.

When the initial speed of HVGT = 75,000 r/min, the high-pressure stage turbine (HT) expansion ratio and the distribution relationship between the low-pressure stage turbine (LT) expansion ratios are the same as the law shown in Figure 7, which will not be analysed in detail here. It is worth pointing out that as the HVGT turbine speed increases and the exhaust flow increases, the low-pressure stage expansion ratio becomes more sensitive to changes in LVGT. With the increase in HVGT turbine speed, when the LVGT blade opening decreases by 10%, the low-pressure turbine expansion ratio increases by about 0.23. The maximum total expansion ratio of the turbine can reach 3.8. Under the premise that the available exhaust energy remains unchanged, the expansion ratio of the two-stage turbine at a high altitude of 5500 m will be greater than 6, and the ultra-high supercharging ratio can be achieved.

The isentropic efficiency of HT and LT is equal to the ratio of the actual process gas's work on the turbine to the maximum available energy of the ideal constant entropy process gas's work on the turbine, namely:

$$\eta_{HT} = \frac{1 - \frac{T_4}{T_3}}{1 - \left(\frac{1}{\pi_{HT}}\right)^{\frac{k_T - 1}{k_T}}} \tag{2}$$

$$\eta_{LT} = \frac{1 - \frac{T_5}{T_4}}{1 - \left(\frac{1}{\pi_{LT}}\right)^{\frac{k_T - 1}{k_T}}} \tag{3}$$

where η_{HT} is the isentropic efficiency of the high-pressure stage turbine, η_{LT} is the isentropic efficiency of the bottom pressure stage turbine, π_{HT} is the expansion ratio of the high-pressure stage turbine, π_{LT} is the expansion ratio of the low-pressure stage turbine, T_3 is the engine cylinder exhaust temperature, T_4 is the exit temperature of the high-pressure stage turbine and T_5 is the exit temperature of the low-pressure stage turbine. It can be seen from the formula that the isentropy efficiency of high- and low-stage turbines is mainly affected by the temperature reduction range and expansion ratio of turbines [26]. For variable-section turbines, turbine expansion ratio and temperature drop are adjusted by VGT blade opening, thus realizing the adjustment of the isentropic efficiency of two-stage turbines. Figure 8 shows the influence of high- and low-pressure VGT blade opening and the turbine expansion ratio on turbine isentropic efficiency during steady-state exhaust flow. As can be seen from the figure, with the increase of VGT blade opening, the efficiency of two-stage turbines presents a trend of first increasing and then decreasing. The maximum efficiency of high-pressure stage turbines appears near 40% of the opening of the HVGT blades, and the maximum efficiency of low-pressure stage turbines appears near 60% of the opening of the LVGT blades.

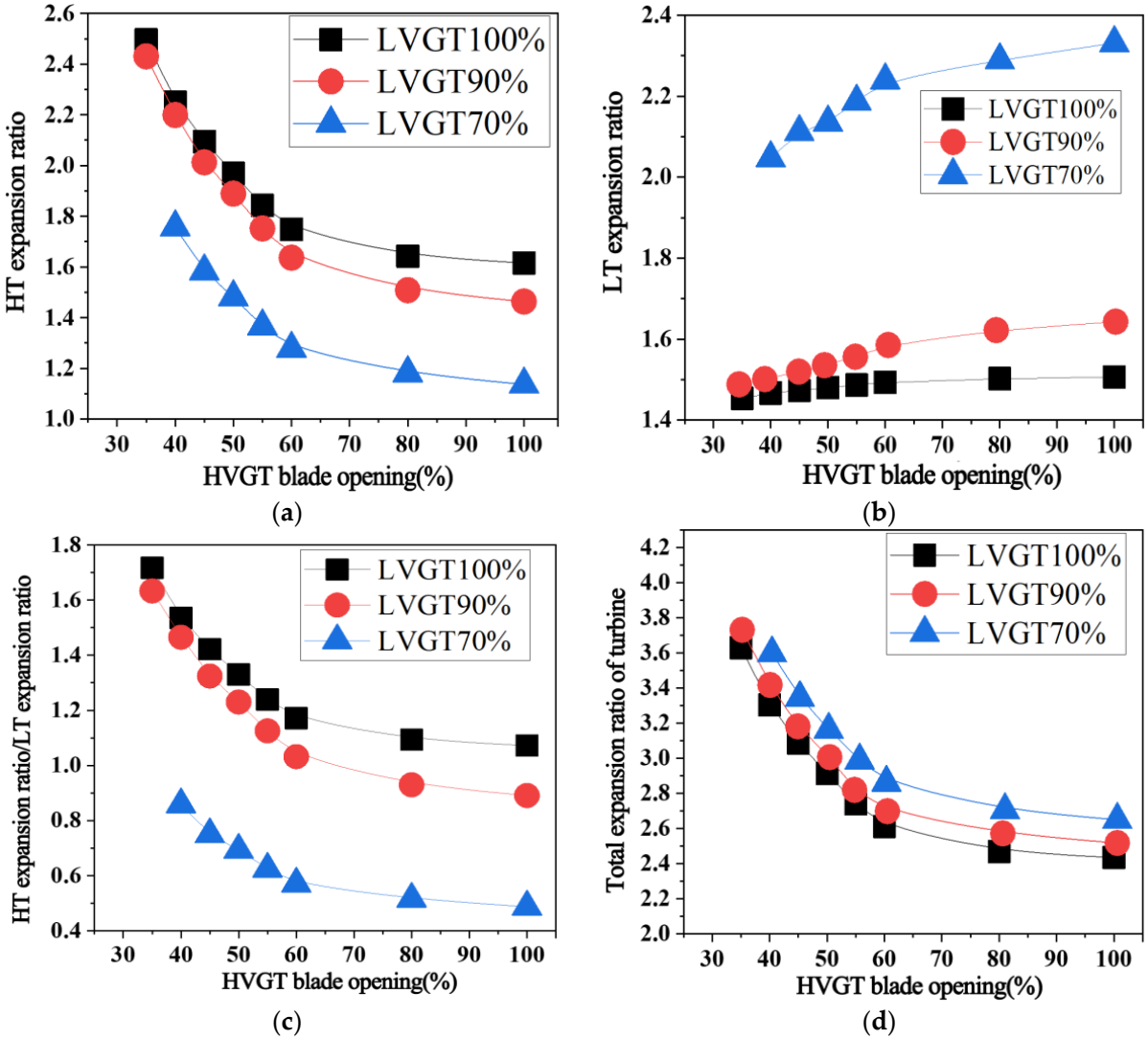


Figure 7. When the initial speed of HVGT is 75,000 r/min, the expansion ratio of high- and low-pressure turbines changes with the opening of VGT blades. (**a**) HT expansion ratio. (**b**) LT expansion ratio. (**c**) The ratio of the expansion ratio of the two-stage turbine. (**d**) Total expansion ratio of turbine.

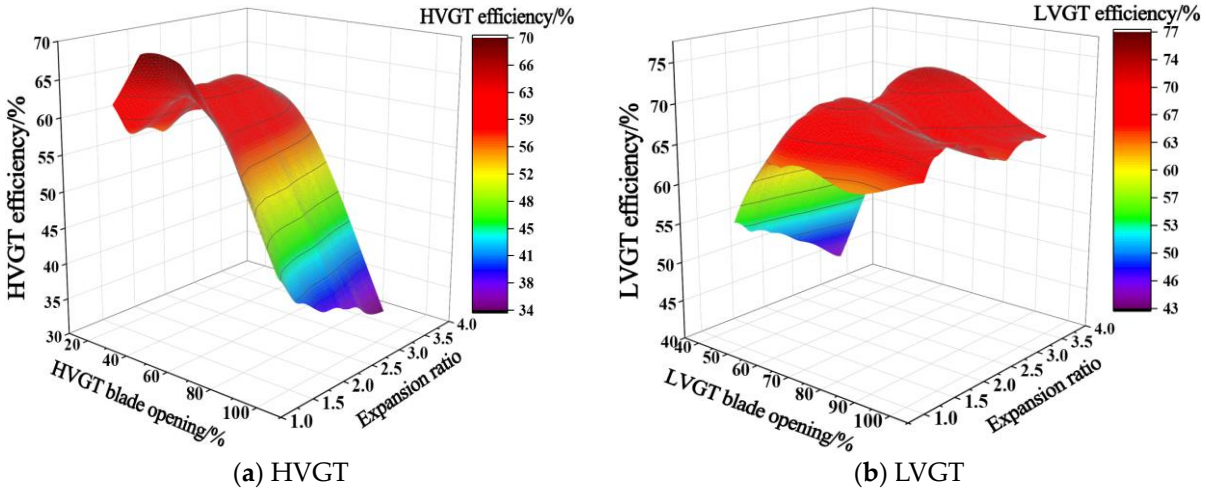
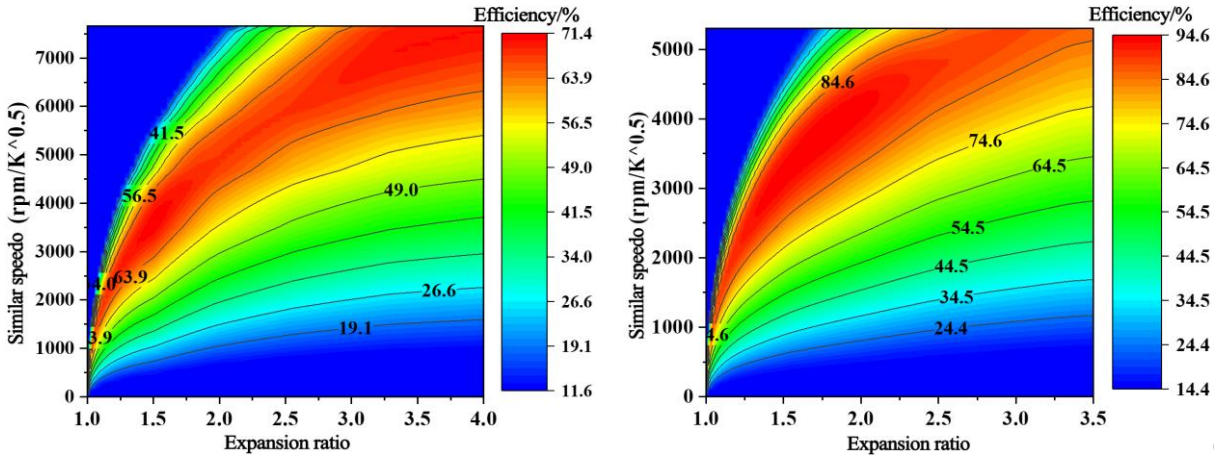


Figure 8. Relationship between VGT vane opening, expansion ratio and turbine efficiency.

Figure 9 shows the relationship between turbine expansion ratio and efficiency corresponding to the optimal opening of VGT blades at high- and low-pressure stages. As can be seen from the figure, when the expansion ratio of high- and low-pressure stage turbines is small, the turbine efficiency range is small. With the increase in the expansion ratio, the maximum efficiency range of HVGT and LVGT turbines expands.



(**a**) HVGT blade opening is 40% (**b**) LVGT blade opening is 60%

Figure 9. Relationship between efficiency, expansion ratio and similar speed of high- and low-pressure stage turbine.

Han Zhiqiang [27] proposed the optimal allocation theory of the expansion ratio of a two-stage adjustable supercharging system based on the principle of equal boost ratio of high- and low-pressure stage and the principle of minimum energy consumption constraint of a two-stage turbine. When the exhaust energy is constant, the change trend of the expansion ratio and total expansion ratio of high- and low-pressure turbines adjusted by the opening of the bypass valve is consistent with this paper. However, under the same expansion ratio, the maximum efficiency range of HVGT and LVGT turbines expands. It can be seen that the dual-VGT system can not only realize the free adjustment of turbine expansion ratio distribution within the full operating range, so as to achieve effective control of supercharge pressure, but can also broaden the maximum efficiency range of turbines.

3.2. Effect of Blade Opening in High- and Low-Pressure VGT on the Turbine Blade Speed Ratio

The isentropic efficiency of turbines is mainly affected by the reaction force and blade speed ratio, in which the reaction force has little influence on the isentropic efficiency. The effect of blade speed ratio u/c^* on the isentropic efficiency can be expressed as $\eta_T = f(u/c^*)$. The blade speed ratio is related to the available energy of the turbine front exhaust and the turbine speed, and the specific approximate formula can be expressed as:

$$\frac{\eta_T}{\eta_{Tmax}} = f(u/c^*) \tag{4}$$

where, η_{Tmax} is the maximum turbine efficiency, u is the impeller linear speed at the inlet of the working impeller and c^* is an ideal speed. Shanghai Jiao Tong University [28] obtained the empirical formula for turbine efficiency by means of a test:

$$\frac{\eta_T}{\eta_{Tmax}} = -0.105 + 2.685(u/c^*) - 0.76(u/c^*)^2 + 1.17(u/c^*)^3 \tag{5}$$

In Formula (5), the linear speeds of high- and low-stage turbines are, respectively:

$$u_{HT} = \pi D_{HT} n_{HT}/60 \tag{6}$$

$$u_{LT} = \pi D_{LT} n_{LT} / 60 \tag{7}$$

where u_{HT}, D_{HT} *and* n_{HT} are the linear speed of the impeller, the diameter of the impeller and the speed of the turbine at the inlet of the working impeller of the high-pressure turbine. And where u_{LT}, D_{LT} *and* n_{LT} are, respectively, the linear speed, diameter and speed of the impeller at the inlet of the working impeller of the low-pressure stage turbine.

The theoretical exit speeds of high- and low-stage turbines are shown in Formulas (8) and (9):

$$c_{HT}^{*} = \sqrt{\frac{2k_T R}{k_T - 1} T_3 [1 - (\frac{1}{\pi_{HT}})^{\frac{k_T - 1}{k_T}}]} \tag{8}$$

$$c_{LT}^{*} = \sqrt{\frac{2k_T R}{k_T - 1} T_4 [1 - (\frac{1}{\pi_{LT}})^{\frac{k_T - 1}{k_T}}]} \tag{9}$$

c_{HT}^{*} is the hypothetical flow rate (m/s) during isentropic expansion of air in high-pressure turbines and c_{LT}^{*} is the hypothetical flow rate (m/s) during isentropic expansion of air in a low-pressure turbine.

The blade speed ratio of high- and low-pressure stage turbines can be obtained with Formulas (6)–(9), as shown in Formulas (10) and (11):

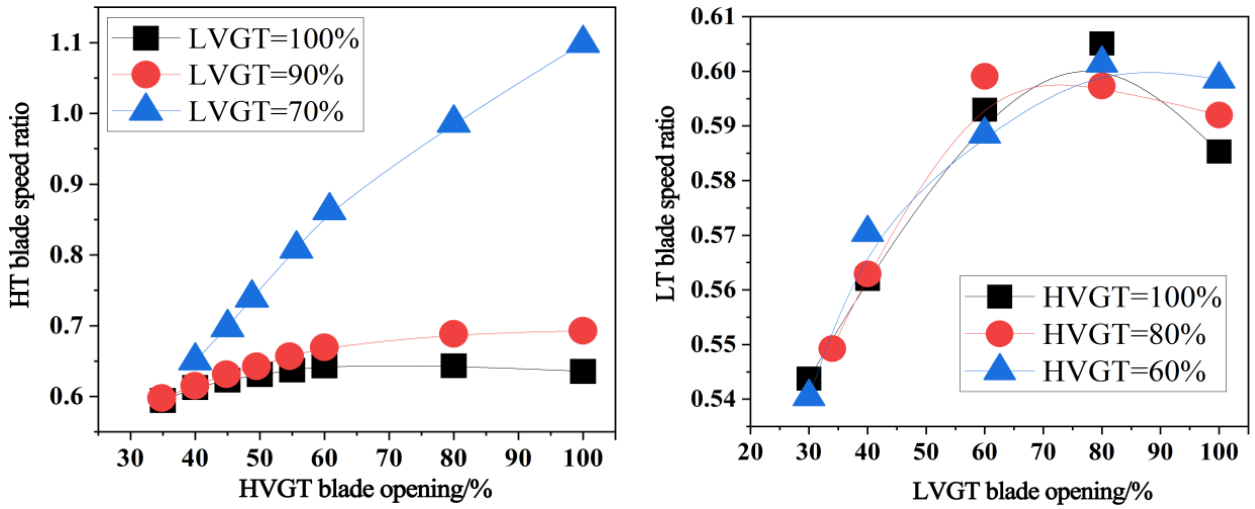
$$\frac{u_{HT}}{c_{HT}^{*}} = \frac{\pi D_{HT} n_{HT}}{60\sqrt{\frac{2k_T R}{k_T - 1} T_5 [1 - (\frac{1}{\pi_{HT}})^{\frac{k_T - 1}{k_T}}]}} \tag{10}$$

$$\frac{u_{LT}}{c_{LT}^{*}} = \frac{\pi D_{LT} n_{LT}}{60\sqrt{\frac{2k_T R}{k_T - 1} T_6 [1 - (\frac{1}{\pi_{LT}})^{\frac{k_T - 1}{k_T}}]}} \tag{11}$$

Figure 10 shows the changing rules of blade speed ratios for high- and low-pressure stage turbines under different VGT blade openings. It can be seen that with the change of the VGT blade opening, the change trend of the blade speed ratio of high- and low-pressure stage turbines is different. This is because the blade opening in HVGT and LVGT has a different influence on the expansion ratio and speed of high- and low-pressure turbines. As shown in Figure 10a, when the LVGT blade opening is 70%, the expansion ratio of the high-pressure stage turbines decreases significantly. At the same time, with the increase in the HVGT blade opening, the expansion ratio of the high-pressure stage turbines further decreases, and the turbine speed decreases slightly, which is reflected in the large increase of u_{HT}/c_{HT}^{*} in Formula (10). However, the blade opening in HVGT has little influence on the expansion ratio of low-pressure stage turbines. With the increase in LVGT blade opening, the low-pressure turbine expansion ratio decreases, while the turbine speed decreases. There is a critical value which makes the low-pressure turbine blade speed ratio reach the maximum value.

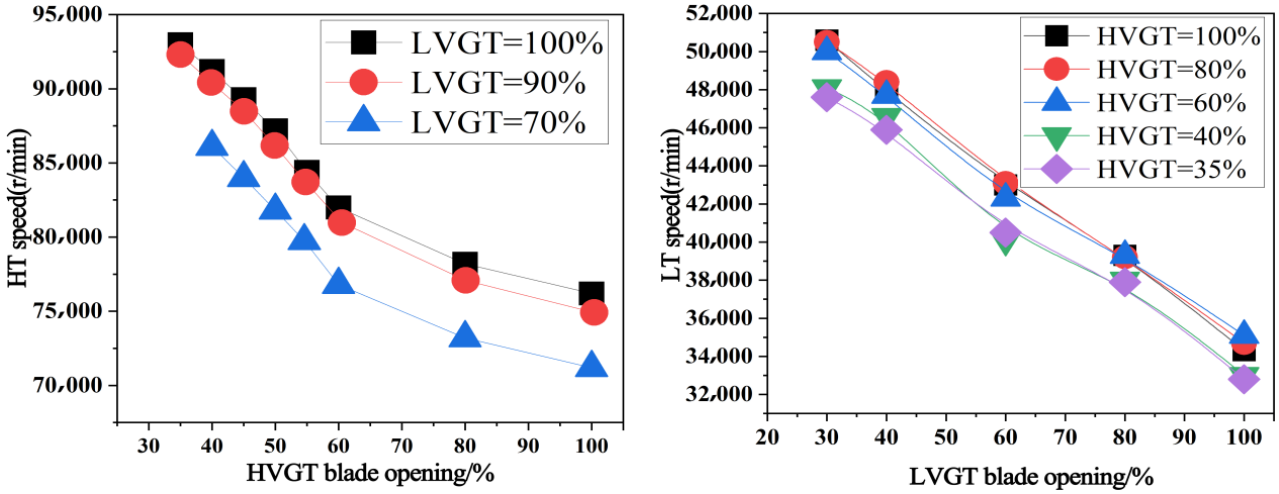
The blade velocity ratio of high- and low-stage turbines is related to turbine speed and enthalpy drop. The effects of VGT blade opening on turbine speed and turbine enthalpy drop will be further analyzed below. As can be seen from Figure 11, as the blade opening of HVGT increases, the speed of high-pressure stage turbines decreases. This is because the enthalpy drop of turbines decreases with the increase in HVGT blade opening, and the power distribution ratio of high-pressure turbines decreases. When the HVGT blade opening is fixed, the HVGT speed decreases as the LVGT blade opening decreases. This is because the opening of LVGT blades decreases, the exhaust resistance of high-pressure turbines increases, the expansion ratio of HVGT decreases and the exhaust energy utilization of high-pressure turbines decreases. As shown in Figure 11b, HVGT blade opening has little influence on the speed of low-pressure stage turbines. The low-pressure turbine speed increases with the decrease in LVGT blade opening. When LVGT blade

opening decreases by 10%, LVGT speed increases by about 2500 r/min, which also explains why the efficiency of low-pressure stage turbines in Figure 10b only changes with LVGT blade opening.



(**a**) HT (**b**) LT

Figure 10. Change rule of high- and low-pressure turbine blade speed ratio with VGT blade opening.



(**a**) HT (**b**) LT

Figure 11. Change rule of high-and low-pressure turbine speed with VGT blade opening.

The specific enthalpy variation trend of high- and low-pressure stage turbines is shown in Figure 12. It can be seen from the figure that the variation trend of specific enthalpy of high- and low-pressure turbines with VGT blade opening is similar to that in Figure 11. In Figure 12a, compared with turbine speed, the specific enthalpy of high-pressure stage turbines decreases faster when the degree of LVGT blade opening is 70%, so the corresponding blade speed ratio of high-pressure stage turbines is larger. Therefore, a conclusion can be drawn that the blade speed ratio of high-pressure stage turbines is affected by both HVGT and LVGT blade opening, while the blade speed ratio of low-pressure stage turbines is only affected by LVGT blade opening. This has important guiding significance for the efficiency adjustment of high- and low-pressure stage turbines under varying altitude and working conditions.

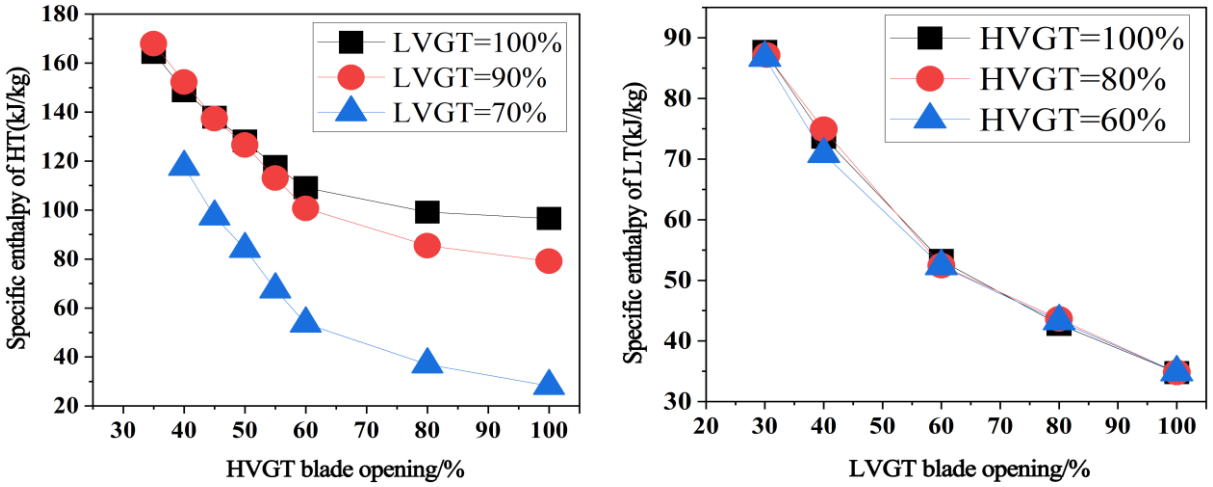


Figure 12. Change rule of specific enthalpy of high- and low-pressure stages with VGT blade opening.

3.3. Influence of Blade Opening of High-and Low-Pressure VGT on Power Consumption and the Isentropic Efficiency of the Compressor

The power consumption of the two-stage compressor is related to the supercharge ratio distribution, the efficiency of the two-stage compressor and the inlet temperature of the two-stage compressor. When the inlet temperatures of high- and low-pressure compressors are different, the ideal supercharge ratio distribution of the two-stage compressor is not equal to 5:5 [29]. Next, the effects of high- and low-pressure VGT blade opening on the supercharge ratio distribution, compressed air temperature and isentropic efficiency of the secondary compressor will be further analyzed.

The change law of intake flow with the opening of HVGT and LVGT blades is similar to that of supercharge pressure. As shown in Figure 13, the intake flow rate decreases with the increase in the HVGT blade opening and increases with the decrease in the LVGT blade opening. This is because there is an energy balance between the compressor and the turbine. As the blade opening of HVGT and LVGT decreases, the speed and total expansion ratio of high- and low-pressure stage turbines increase, and the corresponding intake flow rate increases.

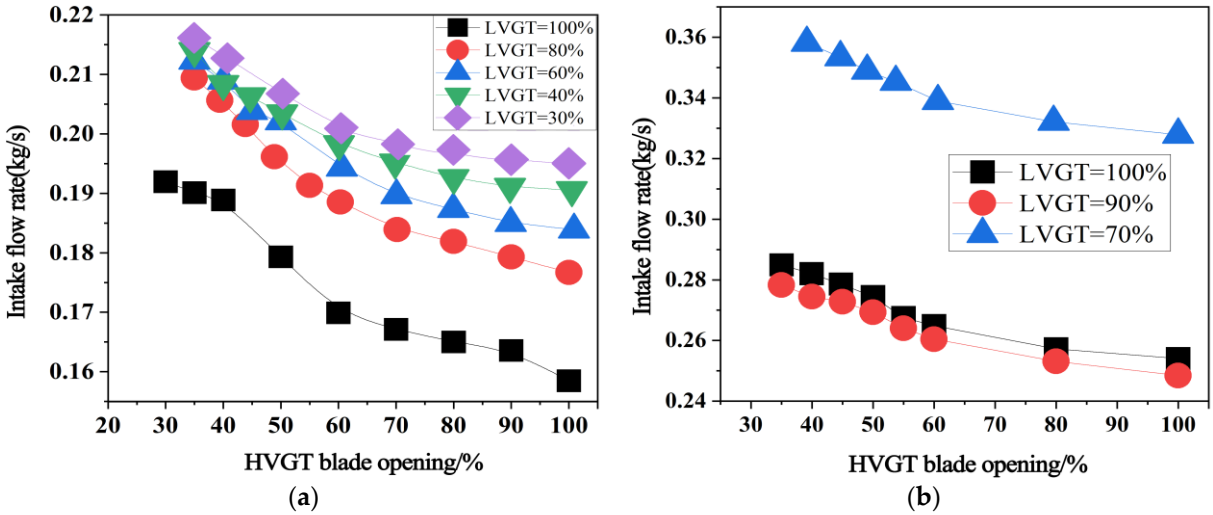


Figure 13. The variation of inlet flow rate with the blade opening of high- and low-pressure VGT. (**a**) The Initial speed of the HVGT is 60,000 r/min. (**b**) The Initial speed of the HVGT is 75,000 r/min.

Figure 14 shows the change of pressure with HVGT blade opening after pressurization of the high-pressure stage at different HVGT speeds (60,000 r/min, 75,000 r/min and 90,000 r/min) when LVGT blade opening is 100%.

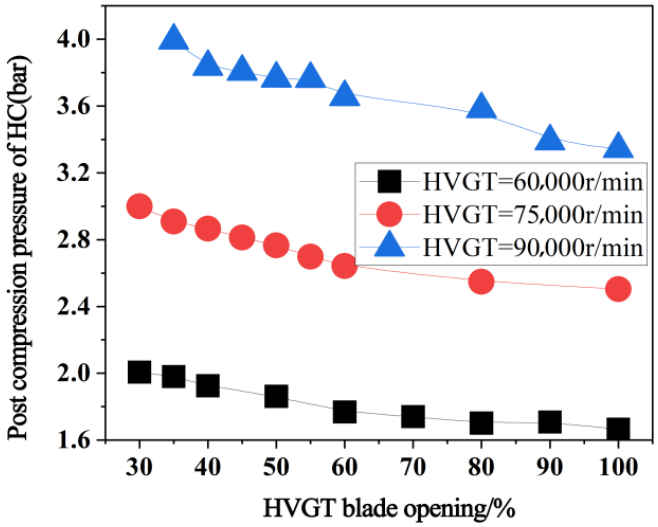


Figure 14. Change rule of boost pressure with HVGT blade opening when LVGT blade opening is at 100%.

By simplifying the formula in the literature [30], the relationship between the boost ratio and turbine expansion ratio in the two-stage supercharging system can be obtained as follows:

$$\pi_c = \left[\frac{\eta_{TC} T_3}{T_0}\left(1 - \pi_T^{\frac{1-k_T}{k_T}}\right) + 1\right]^{\frac{k_c}{k_c - 1}} \tag{12}$$

where π_c is the total supercharge ratio of the two-stage compressor, T_0 is the ambient temperature and k_c is the adiabatic index of the intake air.

As can be seen from Figure 14, under a certain condition of available exhaust energy, as the blade opening of HVGT decreases, the pressurization pressure of the high-pressure stage increases. This is because the total expansion ratio of the turbine increases with the decrease in the HVGT blade opening. When the blade opening of HVGT is reduced from 100% to 30%, the supercharge pressure of the high-pressure stage increases by about 0.5 bar on average. This is because with the increase in available exhaust energy, the HVGT speed increases rapidly, and the supercharge pressure increases significantly.

According to the principle of thermodynamics, the compressed air temperatures of high- and low-pressure compressors are, respectively:

$$T_1 = T_0 \cdot \left[\frac{\pi_{LC}^{(k_c-1)/k_c} - 1}{\eta_{LC}} + 1\right] \tag{13}$$

$$T_2 = T_1 \cdot \left[\frac{\pi_{HC}^{(k_c-1)/k_c} - 1}{\eta_{HC}} + 1\right] \tag{14}$$

In the formula, T_1 is the outlet temperature of the low-pressure compressor, T_2 is the outlet temperature of the high-pressure compressor, η_{LC} is the efficiency of the low-pressure compressor, η_{HC} is the efficiency of the high-pressure compressor and π_{HC} and π_{LC} are the pressurization ratio of the high- and low-pressure compressor, respectively.

The outlet temperature of high- and low-pressure compressor is affected by the supercharge ratio, the inlet temperature and the efficiency of the supercharger. The temperature changes with the HVGT blade opening after compression of the low-pressure compressor are shown in Figure 15. As can be seen from the figure, with the increase in HVGT blade

opening, the temperature change after the low-pressure stage pressure is not obvious, and the overall trend is first an increase and then a decrease. However, with the decrease in LVGT blade opening, the power capacity of low-pressure stage turbines increases. When the LVGT blade opening is in the range of 30%~60%, the temperature increase after low-pressure stage pressure is particularly obvious. The temperature after high-pressure stage compressor changes significantly with the blade opening of HVGT, as shown in Figure 15b. With the increase in the HVGT blade opening, the temperature after high-pressure stage pressure decreases, and when the LVGT blade opening is large, the temperature after high-pressure stage pressure changes obviously with the HVGT opening. When the HVGT blade opening is in the range of 60%~100%, the temperature after high-pressure stage pressure changes obviously with the HVGT blade opening.

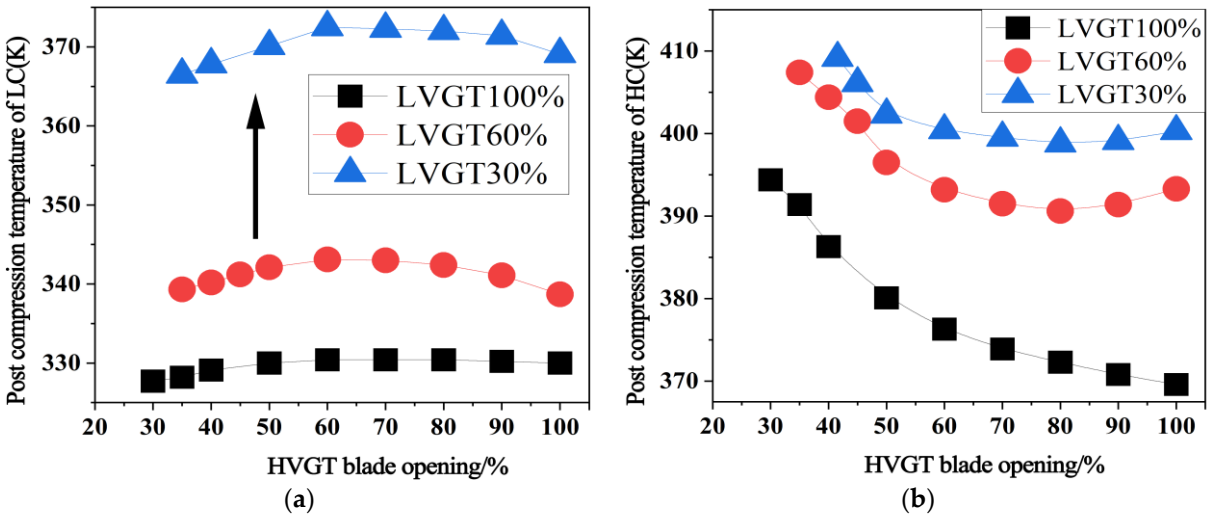


Figure 15. When the initial speed of HVGT is 60,000 r/min, the temperature of the two-stage compressor after compression changes with the opening of HVGT. (**a**) Post compression temperature of LC. (**b**) Post compression temperature of HC.

When the initial speed of HVGT = 75,000 r/min, the changes of key parameters of the high- and low-pressure compressor with VGT blade opening are shown in Figure 16. Figure 16a shows that the variation of temperature after high-pressure stage with HVGT blade opening is similar to that of Figure 15b. When LVGT blade opening decreases, the higher the available energy of the exhaust, the stronger the work energy of the low-pressure stage turbine, and the greater the rising trend of the supercharging ratio. When the LVGT blade opening is 70%, compared with when the LVGT blade opening is 90%, the temperature after high-pressure-stage compression is increased by an average of 60 K. The increase in air temperature after high-pressure-stage compression is mainly affected by the temperature and supercharge ratio before high-pressure-stage compression. It can be seen from Figure 16b that with the decrease in LVGT blade opening, the pressurization ratio of the low-pressure stage increases, and the temperature after low-pressure stage pressure increases significantly.

In Figure 16f, the ratio of high- and low-pressure booster ratios is the same as the change trend of the ratio of the turbine expansion ratio with the change trend of the VGT blade opening. As the blade opening of HVGT decreases, the turbocharging ratio of high-pressure stage increases, while that of low-pressure stage remains basically unchanged, and the ratio of turbocharging ratio increases slowly. With the decrease of LVGT blade opening, the pressurization ratio of low-pressure stage turbines increases, while the pressurization ratio of high-pressure stage turbines decreases, and the ratio of pressurization ratio decreases rapidly.

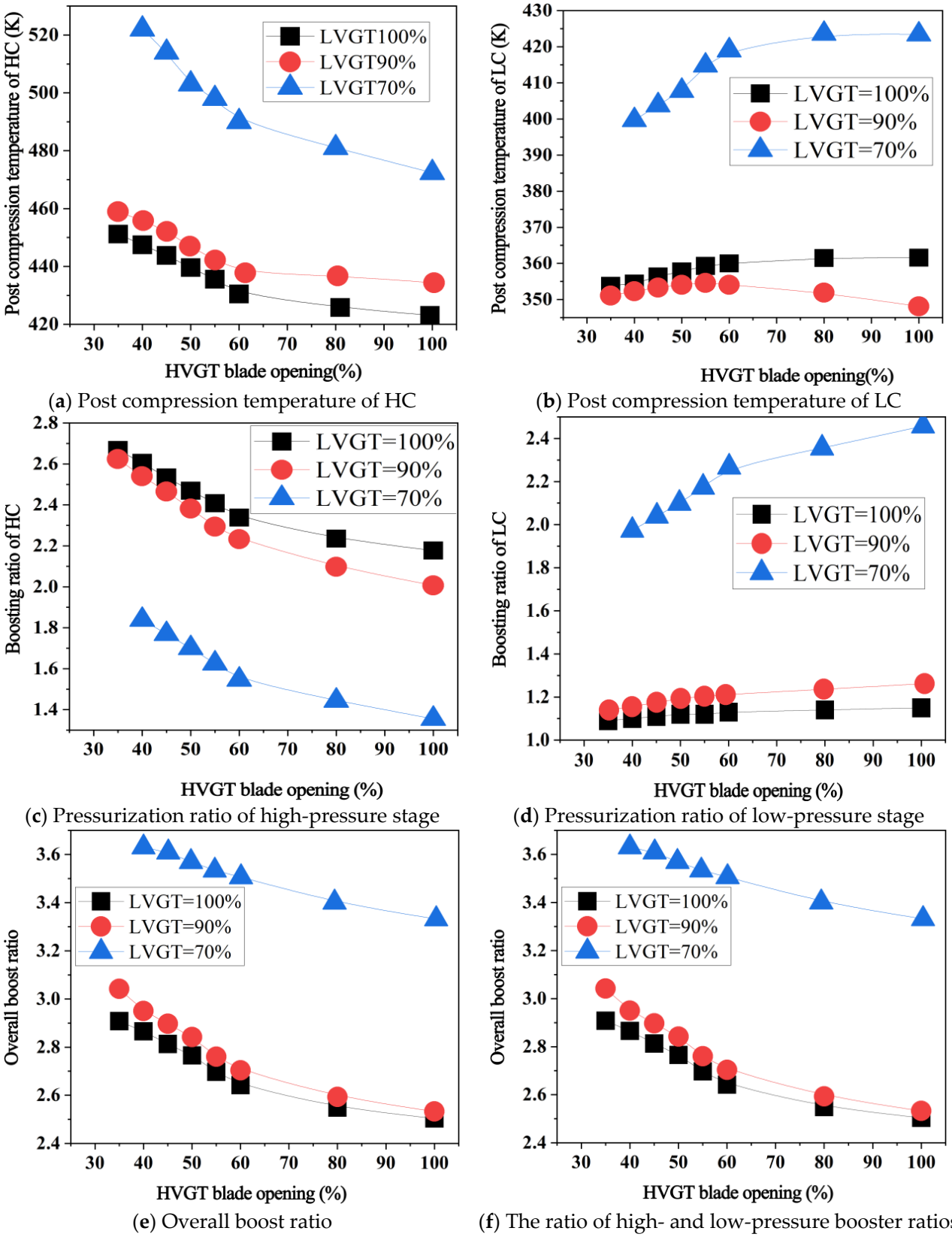


Figure 16. Changes of high- and low-pressure stage compressor parameters with VGT vanes opening when HVGT initial speed at 75,000 r/min.

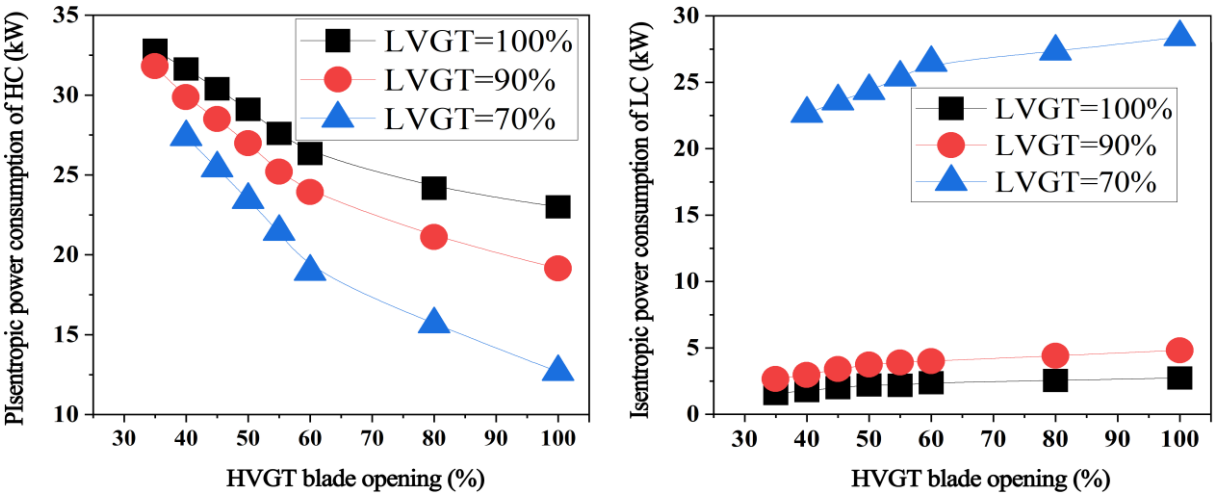
According to the double-VGT two-stage variable turbine flow characteristics test system, the test analysis was carried out, and the isentropy work consumption of high- and low-pressure compressors was determined, respectively, as follows:

$$E_{HC} = m_c \frac{k_c}{k_c - 1} RT_1 \left[(\pi_{HC})^{\frac{k_c - 1}{k_c}} - 1 \right] \tag{15}$$

$$E_{LC} = m_c \frac{k_c}{k_c - 1} RT_0 \left[(\pi_{LC})^{\frac{k_c - 1}{k_c}} - 1 \right] \tag{16}$$

where E_{HC} and E_{LC} are the isentropic work consumption of high- and low-pressure compressors, respectively. π_{HC} and π_{LC} are the pressurization ratios of high- and low-pressure compressors, respectively, and m_c is the intake mass flow rate (kg/s).

The power consumption variation trend of high- and low-pressure compressor calculated according to Formulas (15) and (16) is shown in Figure 17. It can be seen from Figure 17a that as the blade opening of HVGT decreases, the power consumption of the high-pressure compressor increases. When the blade opening in HVGT is in the range of 60 to 100%, the power consumption of the high-pressure compressor increases significantly with the increase in LVGT blade opening. This is because the back pressure of the high-pressure stage turbines is reduced, the work capacity of the high-pressure stage turbines is enhanced and the work consumption of the high-pressure stage compressors is increased.



(**a**) HC (**b**) LC

Figure 17. Variation of isentropic power consumption of high- and low-pressure stage compressor with VGT vanes opening.

Tianjin University [31] proposed that the minimum total drive work of a two-stage compressor can be obtained by reasonably controlling the strength of the intercooler, the pressure ratio distribution and the operation efficiency of the two-stage compressor. However, in the variable altitude environment, as the compressor inlet pressure and temperature decrease, the target supercharge ratio and compressor efficiency decrease under the matching working conditions, and the supercharge ratio distribution in the plain environment will not be effective [32]. It can be seen that there is a minimum value of the dissipated work of the two-stage compressor under the variable-altitude non-matching condition, and the corresponding supercharge ratio distribution and compressor inlet temperature are the best. However, in the polytropic compression process of the two-stage supercharging system, the distribution of the supercharging ratio, the intercooling strength, the operation efficiency of the two-stage compressor and the distribution of the turbine expansion ratio are related to the environmental parameters, and further research

is needed to obtain the minimum power consumption of the two-stage compressor at the corresponding altitude.

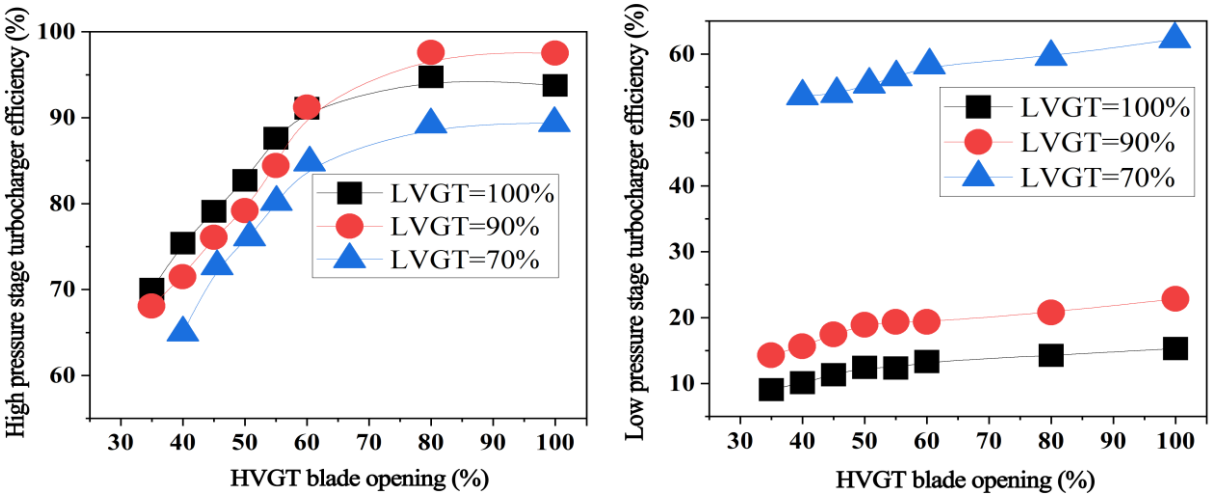
According to the double-VGT two-stage variable turbine flow characteristics test system, the test analysis is conducted, and the isentropy efficiency of the high- and low-pressure supercharger is determined as follows:

$$\eta_{HTC} = \frac{\Delta h_{1\sim2}}{\Delta h_{3\sim4}} = \frac{\frac{k_T RT_3^*}{k_T-1}\left[1-\left(\frac{1}{\pi_{HT}}\right)^{\frac{k_T-1}{k_T}}\right]}{\frac{k_c}{k_c-1}RT_1\left[\left(\pi_{HC}\right)^{\frac{k_c-1}{k_c}}-1\right]} \tag{17}$$

$$\eta_{LTC} = \frac{\Delta h_{0\sim1}}{\Delta h_{4\sim5}} == \frac{\frac{k_T RT_4^*}{k_T-1}\left[1-\left(\frac{1}{\pi_{LT}}\right)^{\frac{k_T-1}{k_T}}\right]}{\frac{k_c}{k_c-1}RT_0\left[\left(\pi_{LC}\right)^{\frac{k_c-1}{k_c}}-1\right]} \tag{18}$$

where η_{HTC} and η_{LTC} are the isentropic efficiency of high- and low-pressure supercharger, respectively. π_{HT} and π_{LT} are, respectively, the expansion ratios of high- and low-pressure stage turbines. $\Delta h_{1\sim2}$ and $\Delta h_{0\sim1}$ are, respectively, the isentropic enthalpy rise of high- and low-pressure stage compressors; $\Delta h_{3\sim4}$ and $\Delta h_{4\sim5}$ indicate the isentropic enthalpy drop of high- and low-stage turbines, respectively.

According to Formulas (17) and (18), the variation rules for the efficiency of the high- and low-pressure supercharger and the opening of the VGT blade are obtained (as shown in Figure 18). Among them, when the HVGT blade opening is between 30% and 60%, the efficiency of high-pressure stage turbines increases rapidly with the increase in HVGT blade opening. When the HVGT opening is 60%~100%, the efficiency of the high- pressure supercharger increases slowly with the HVGT blade opening. The efficiency of the low-pressure turbine varies significantly with the blade opening of LVGT. Compared with an LVGT blade opening of 100%, when LVGT blade opening is 70%, the low-pressure stage turbine efficiency increases from 10% to more than 50%, which proves that low-pressure stage turbines have enhanced exhaust energy utilization.



(**a**) High-pressure stage supercharger (**b**) Low-pressure stage supercharger

Figure 18. The efficiency of the high- and low-pressure stage superchargers vary with the blade opening of VGT.

Liu [33] found that the efficiency of the two-stage supercharger with a bypass valve was determined by the efficiency and enthalpy drop distribution of the high- and low-voltage supercharger, and proposed the principle of "matching the exhaust energy distribution with the efficiency of the supercharger". However, the flow range of the high efficiency zone of

the ordinary-bypass-type two-stage supercharging system is narrow, and the turbine bypass valve is opened in the middle- and high-speed zone of the diesel engine. The regulation of the flow area of two-stage turbines on enthalpy drop and the expansion ratio of variable-altitude turbines does not match the efficiency of two-stage turbines. The bypass valve throttling results in a large loss of available exhaust energy, and the low-pressure turbine cannot effectively use the bypass exhaust energy [34]. The double-VGT turbocharging system can freely adjust the flow area of high- and low-pressure stage turbines through the opening of VGT blades, meeting the requirements of target boost pressure, expansion ratio distribution, boost ratio distribution and isentropic efficiency for superchargers under different environmental conditions, and enhancing the exhaust energy utilization rate of low-pressure stage turbines. Therefore, compared with other supercharging systems, the dual-VGT supercharging system is an important way to achieve high-efficiency operation of internal combustion engines with variable altitudes and full working conditions.

4. Conclusions

In this paper, a two-stage VGT variable turbine flow characteristics test system was designed and developed, and the flow characteristics of two-stage variable turbines were studied. The effects of blade opening of high- and low-pressure VGT stages on available energy distribution, overall expansion ratio, blade velocity ratio and turbine efficiency were explored. Specific conclusions are as follows:

(1) Different degrees of LVGT blade opening have different influences on the available energy of high-pressure stage exhaust gas. With the decrease in LVGT blade opening, the available energy of high-pressure stage exhaust gas increases. Different degrees of LVGT blade opening have different influences on the available energy of high-pressure turbine exhaust. As the blade opening of LVGT decreases, the back pressure of the high-pressure stage turbine increases, the pressure and temperature in front of the high-pressure stage turbine increase and the available exhaust energy increases. The total expansion ratio of two-stage turbines increases with the decrease in blade opening of HVGT and LVGT. When HVGT blade opening is in the range of 60% to 100%, LVGT blade opening has a greater influence on the total expansion ratio, while when HVGT blade opening is in the range of 30% to 60%, HVGT blade opening has a greater influence on the total expansion ratio;

(2) The blade speed ratio of HT is affected by the blade opening of HVGT and LVGT. However, the blade speed ratio of LT is only affected by the blade opening of LVGT. The research results have important guiding significance for the efficiency adjustment of HT and LT under varying altitude and working conditions;

(3) High-pressure-stage compressor power consumption of the high-pressure stage increases with the decrease in the blade opening of HVGT. When the blade opening of HVGT is in the range of 60% to 100%, with the increase in the blade opening of LVGT, the pressure reduction of the high-pressure stage vortex back is small. The power capacity of the high-pressure stage turbine is enhanced and the power consumption of the high-pressure stage compressor is increased significantly. The efficiency of low-pressure stage turbines varies significantly with LVGT blade opening. Compared with an LVGT opening of 100%, when the LVGT opening is 70%, the efficiency of low-pressure stage turbines increases from 10% to more than 50%, which proves that the low-pressure stage turbines are in good alignment. With the increase in HVGT blade opening, the HVGT turbine efficiency increases rapidly when the HVGT opening is between 30% and 60%, while the HVGT supercharger efficiency increases slowly when the HVGT opening is between 60% and 100%.

Author Contributions: Formal analysis, X.Z.; Investigation, H.Z.; Resources, S.D. and J.C.; Data curation, G.Z.; Writing—original draft, Q.P.; Writing—review & editing, Z.Z.; Project administration, R.L. All authors have read and agreed to the published version of the manuscript.

Funding: The authors would like to acknowledge the support of the National Natural Science Foundation of China (No. 52106192).

Data Availability Statement: Data are contained within the article.

Conflicts of Interest: Jun Cai was employed by the company Jiangsu Kaidi Navigation Control System Limited Company. The remaining authors declare that the research was conducted in the absence of any commercial or financial relationships that could be construed as a potential conflict of interest.

Nomenclature

Notations

Δh_{adT}	Isentropic enthalpy drop of the turbine
k_T	Exhaust adiabatic index
T_3^*	Cylinder exhaust temperature
R	Gas constant
D	Diameter of the impeller
n	Speed of the turbine
c^*	Ideal speed
k_c	Adiabatic index of the intake air.
m_c	Intake mass flow rate
u	Linear speed of the impeller
π_c	The total supercharge ratio of the two-stage compressor
π_{HC}	The pressurization ratio of the high-pressure compressor
π_{LC}	The pressurization ratio of the low-pressure compressor
π_T	The total expansion ratio of the two-stage turbine
π_{HT}	The expansion ratio of the high-pressure stage turbine
π_{LT}	The expansion ratio of the low-pressure stage turbine
E_{HC}	The isentropic work consumption of high-pressure compressors
E_{LC}	The isentropic work consumption of low-pressure compressors
η_{Tmax}	The maximum turbine efficiency
η_{LC}	The efficiency of the low-pressure compressor
η_{HC}	The efficiency of the high-pressure compressor
η_{HTC}	The isentropic efficiency of the high-pressure supercharger
η_{LTC}	The isentropic efficiency of the low-pressure supercharger
$\Delta h_{0\sim1}$	The isentropic enthalpy rise of low-pressure stage compressors
$\Delta h_{1\sim2}$	The isentropic enthalpy rise of high-pressure stage compressors
$\Delta h_{3\sim4}$	The isentropic enthalpy drop of high stage turbines
$\Delta h_{4\sim5}$	The isentropic enthalpy drop of low stage turbines
T_0	Ambient temperature
T_1	Outlet temperature of the low-pressure compressor
T_2	Outlet temperature of the high-pressure compressor
T_3	Engine cylinder exhaust temperature
T_4	Exit temperature of the high-pressure stage turbine
T_5	Exit temperature of the low-pressure stage turbine

Abbreviation

VGT	Variable-geometry Turbocharge
ICE	Internal combustion engine
Twin-VGT	Twin variable-geometry turbocharging
HVGT	High variable-geometry turbocharging
LVGT	Low variable-geometry turbocharging
HT	High-pressure stage turbine
LT	Low-pressure stage turbine
HC	High-pressure stage compressor
LC	Low-pressure stage compressor
BSFC	Brake specific fuel consumption

References

1. Rawat, S.; Patchappalam, K.; Sahare, A. TCV-A unique solution for HD commercial BSIV diesel engine for range of altitude operation. *SAE Int. J. Engines* **2017**, *10*, 9–16. [CrossRef]
2. Liu, R.-L.; Zhang, Z.-J.; Jiao, Y.-F.; Yang, C.-H.; Zhang, W.-J. Study on flight performance of propeller-driven UAV. *Int. J. Aerosp. Eng.* **2019**, *2019*, 6282451. [CrossRef]
3. Ramos, Á.; García-Contreras, R.; Armas, O. Performance, combustion timing and emissions from a light duty vehicle at different altitudes fueled with animal fat biodiesel, GTL and diesel fuels. *Appl. Energy* **2016**, *182*, 507–517. [CrossRef]
4. Szedlmayer, M.; Kweon, C. Effect of Altitude Conditions on Combustion and Performance of a Multi-Cylinder Turbocharged Direct-Injection Diesel Engine. In Proceedings of the SAE 2016 World Congress and Exhibition, Detroit, MI, USA, 12–14 April 2016.
5. Liu, R.; Lin, C.; Dong, S.; Zhang, Z.; Xu, X.; Zhou, G. High Altitude Calibration Test of Two-stage Adjustable Supercharging System of Diesel Engine. *Trans. CSICE* **2016**, *34*, 543–548.
6. Liu, R. *Research on Environmental Adaptability of Diesel Engines at Plateau*; Beijing Institute of Technology Press: Beijing, China, 2013.
7. Wu, G.; Zhang, H.; Wei, M. Numerical Calculation and Analysis of High Altitude Characteristics of Centrifugal Compressor. *Veh. Power Technol.* **2014**, *4*, 1–5.
8. Li, Z.; Zheng, X. Review of design optimization methods for turbomachinery aerodynamics. *Prog. Aerosp. Sci.* **2017**, *93*, 1–23. [CrossRef]
9. Carlucci, A.P.; Ficarella, A.; Laforgia, D.; Renna, A. Supercharging system behavior for high altitude operation of an aircraft 2-stroke Diesel engine. *Energy Convers. Manag.* **2015**, *101*, 470–480. [CrossRef]
10. Wang, Y. Study on Effect of Reynolds Number on Performance of Centrifugal Compressor. Master's Thesis, Harbin Institute of Technology, Harbin, China, 2012.
11. Zhao, R.; Zhuge, W.; Zhang, Y.; Yang, M.; Martinez-Botas, R.; Yin, Y. Study of two-stage turbine characteristic and its influence on turbo-compound engine performance. *Energy Convers. Manag.* **2015**, *95*, 414–423. [CrossRef]
12. Zhang, Z.; Liu, R.; Dong, S.; Zhou, G.; Liu, W.; Peng, Q. Thermodynamic cycle characteristics of twin-VGT diesel engine and its control method at variable altitudes. *Appl. Therm. Eng.* **2022**, *211*, 118429. [CrossRef]
13. Yao, Y.; Shi, L.; Zhang, Z.; Xiao, M.; Liu, M.; Tan, J. *Research of the High Altitude Control Strategy of the Piston Aero-Engine Using Two-Stage Turbocharger Coupled with Single Supercharging System*; SAE Technical Paper; SAE International: Warrendale, PA, USA, 2019.
14. Liu, R.; Zhang, Z.; Dong, S.; Zhou, G. High-Altitude Matching Characteristic of Regulated Two-Stage Turbocharger with Diesel Engine. *J. Eng. Gas Turbines Power Trans. ASME* **2017**, *139*, 094501. [CrossRef]
15. Kovacs, D.; Eilts, P. *Potentials of Miller Cycle on HD Diesel Engines Using a 2-Stage Turbocharging*; SAE Technical Paper; SAE International: Warrendale, PA, USA, 2018.
16. Li, C. Matching and Regulation of Adjustable Two-Stage Supercharging System of Diesel Engine at Plateau. Master's Thesis, Beijing Institute of Technology, Beijing, China, 2016.
17. Llamas, X.; Eriksson, L. Control-oriented compressor model with adiabatic efficiency extrapolation. *SAE Int. J. Engines* **2017**, *10*, 1903–1916. [CrossRef]
18. Kozak, D.; Mazuro, P. Numerical Analysis of Two-Stage Turbine System for Multicylinder Engine under Pulse Flow Conditions with High Pressure-Ratio Turbine Rotor. *Energies* **2023**, *16*, 751. [CrossRef]
19. Zhang, H.; Tang, X.; Mu, L.; Shi, L.; Deng, K. Theoretical and experimental investigation of the pressure ratio distribution and the regulation strategy of a two-stage turbocharging system for various altitudes operation. *J. Mech. Sci. Technol.* **2021**, *35*, 1251–1265. [CrossRef]
20. *JB/T9752.1-2005*; Turbochargers Part 1: General Technical Conditions. National Development and Reform Commission (NDRC): Beijing, China, 2005.
21. *JB/T9752.2-2005*; Turbochargers Part 2: Test Methods. National Development and Reform Commission (NDRC): Beijing, China, 2005.
22. Kozak, D.; Mazuro, P.; Teodorczyk, A. Numerical simulation of two-stage variable geometry turbine. *Energies* **2021**, *14*, 5349. [CrossRef]
23. Thomasson, A.; Leufvén, O.; Criscuolo, I.; Eriksson, L. Modeling and validation of a boost pressure actuation system, for a series sequentially turbocharged SI engine. *Control. Eng. Pract.* **2013**, *21*, 1860–1870. [CrossRef]
24. Li, H.; Shi, L.; Deng, K. Research on the power recovery of diesel engines with regulated two-stage turbocharging system at different altitudes. *Int. J. Rotating Mach.* **2014**, *2014*, 209084. [CrossRef]
25. Yang, M.; Gu, Y.; Deng, K.; Yang, Z.; Liu, S. Influence of altitude on two-stage turbocharging system in a heavy-duty diesel engine based on analysis of available flow energy. *Appl. Therm. Eng.* **2018**, *129*, 12–21. [CrossRef]
26. Liu, Y. Systematic Optimization and Control Design for Downsized Boosted Engines with Advanced Turbochargers. Master's Thesis, The Ohio State University, Columbus, OH, USA, 2014.
27. Han, Z. Study on parameter selection of two-stage supercharging system and its influence on combustion process. Ph.D. Thesis, Tianjin University, Tianjin, China, 2013.
28. Li, H.; Zhang, G.; Zhang, H.; Shi, L.; Yang, M.; Deng, K. Equivalent matching model of a regulated two-stage turbocharging system for the plateau adaptability. *Proc. Inst. Mech. Eng. Part D J. Automob. Eng.* **2016**, *230*, 1654–1669. [CrossRef]

29. Song, Y.; Xu, Y.; Cheng, X.; Wang, Z.; Zhu, W.; Fan, X. Using a Genetic Algorithm to Achieve Optimal Matching between PMEP and Diameter of Intake and Exhaust Throat of a High-Boost-Ratio Engine. *Energies* **2022**, *15*, 1607. [CrossRef]
30. Rathod, D.; Xu, B.; Filipi, Z.; Hoffman, M. An experimentally validated, energy focused, optimal control strategy for an Organic Rankine Cycle waste heat recovery system. *Appl. Energy* **2019**, *256*, 113991. [CrossRef]
31. Wu, B.; Han, Z.; Yu, X.; Zhang, S.; Nie, X.; Su, W. A method for matching two-stage turbocharger system and its influence on engine performance. *J. Eng. Gas Turbines Power* **2019**, *141*, 054502. [CrossRef]
32. Shi, X.; Wang, T.; Ma, C. Simulations of the diesel engine performance with a two-stage sequential turbocharging system at different altitudes. *Proc. Inst. Mech. Eng. Part D J. Automob. Eng.* **2014**, *228*, 1718–1726. [CrossRef]
33. Liu, B.; Deng, K.Y.; Cui, Y. Equivalent turbocharger model of regulated two-stage turbocharging system. *J. Energy Inst.* **2010**, *83*, 195–201. [CrossRef]
34. Zhu, D.; Sun, Z.; Zheng, X. Turbocharging strategy among variable geometry turbine, two-stage turbine, and asymmetric two-scroll turbine for energy and emission in diesel engines. *Proc. Inst. Mech. Eng. Part A J. Power Energy* **2020**, *234*, 900–914. [CrossRef]

Disclaimer/Publisher's Note: The statements, opinions and data contained in all publications are solely those of the individual author(s) and contributor(s) and not of MDPI and/or the editor(s). MDPI and/or the editor(s) disclaim responsibility for any injury to people or property resulting from any ideas, methods, instructions or products referred to in the content.